Pergamon

*Journal of Structural Geology*, Vol. 20, No. 9/10, pp. 1155 to 1168, 1998

0191-8141/98/$ - see front matter

PII: S0191-8141(98)00063-7

# Magma traps and driving pressure: consequences for pluton shape and emplacement in an extensional regime

JOHN P. HOGAN*, JONATHAN D. PRICE and M. CHARLES GILBERT

University of Oklahoma, School of Geology and Geophysics, Sarkey's Energy Center, Rm 810, Norman, OK, 73019-0628, U.S.A.

(*Received* 18 *August* 1997; *accepted in revised form* 20 *April* 1998)

**Abstract**—The level of emplacement and final form of felsic and mafic igneous rocks of the Wichita Mountains Igneous Province, southwestern Oklahoma, U.S.A. are discussed in light of magma driving pressure, lithostatic load, and crustal magma traps. Deposition of voluminous A-type rhyolites upon an eroded gabbroic substrate formed a subhorizontal strength anisotropy that acted as a crustal magma trap for subsequent rising felsic and mafic magma. Intruded along this crustal magma trap are the A-type sheet granites (length/thickness 100:1) of the Wichita Granite Group, of which the Mount Scott Granite sheet is typical, and smaller plutons of biotite bearing Roosevelt Gabbro. In marked contrast to the subhorizontal granite sheets, the gabbro plutons form more equant stocks with flat roofs and steep side walls. Late Diabase dikes cross-cut all other units, but accompanying basaltic flows are extremely rare in the volcanic pile.

Based on magmastatic calculations, we draw the following conclusions concerning the level of emplacement and the shape of these intrusions. (1) Magma can rise to a depth at which the magma driving pressure becomes negligible. Magma that maintains a positive driving pressure at the surface has the potential to erupt. (2) Magma ascent may be arrested at a deeper level in the crust by a subhorizontal strength anisotropy (i.e. crustal magma trap) if the magma driving pressure is greater than or equal to the lithostatic load at the depth of the subhorizontal strength anisotropy. (3) Subhorizontal sheet-intrusions form along crustal magma traps when the magma driving pressure greatly exceeds the lithostatic load. Under such conditions, the magma driving pressure is sufficent to lift the overburden to create the necessary space for the intrusion. (4) Thicker steep-sided stocks or batholiths, with flat roofs, form at crustal magma traps when the magma driving pressure approximates that of the lithostatic load. Under these conditions, the necessary space for the intrusion must be created by other mechanisms (e.g. stoping). (5) Subvertical sheets (i.e. dikes) form when the magma driving pressure is less than the lithostatic load at the level of emplacement. 

## INTRODUCTION

*"Field studies are showing that many of these bottomless batholiths rest in places on visible floors of older rocks. There is evidence of much lateral movement by the magma which has formed sheetlike, tack-shaped, or tonguelike masses ..."* (Chamberlin and Link, 1927)

*"Even gigantic bodies of magma have been intruded as sheets as, for example, in the Sudbury and Bushveld masses, ... but these are of basic material. The great granite masses do not exhibit a sheet form ..."* (Read, 1948)

These quotes define a theme central to understanding the origin of granite: the shape of igneous intrusions. Chamberlin and Link (1927) challenged the dogma that granite batholiths continue to great depths, ever widening, and ever increasing in size, with the suggestion that large volumes of granitic magma crystallize as nearly subhorizontal sheets. However, Read (1948) in his famous paper 'Granites and Granites' re-emphasized the conventional view of granite batholiths as large intrusions having "*no known floor*" (e.g. Bates and Jackson, 1980). This controversy was revisited with vigor by Hamilton and Myers (1974a, b) who presented a case for the Boulder Batholith, Montana as a thin, floored sheet, whereas Klepper *et al.* (1974) emphasized the vertical rather than the horizontal aspects of the intrusion and considered the batholith had to widen downward to great depths. Even today a consensus on the shape of granitic batholiths has yet to be reached. Whether granitic batholiths extend as vertical columns widening downward toward the base of the crust (e.g. Paterson *et al.*, 1996, fig. 8) or are flat-bottomed tabular sheets with high aspect ratios (e.g. Petford, 1996, fig. 9; McCaffrey and Petford, 1997) remains the subject of considerable debate.

This paper discusses shapes of felsic and mafic, shallow-level intrusions emplaced in an extensional regime. Among a plethora of variables contributing to determination of the level of emplacement and of the final shape of an intrusion we choose to explore the role of two: (1) magma driving pressure (Baer and Reches, 1991), and (2) crustal magma traps (Hogan and Gilbert, 1995). We fully recognize the complexity and diversity encompassed by the statement "*There are granites and there are granites*" which is as true today as it was when coined at the first granite symposium (which this issue commemorates) by H. H. Read. The model presented is heuristic, with the intent to promote further debate on the significance of the shapes of intrusions, an issue central to the origin of granite.

*Now at: Department of Geology and geophysics, 125 McNutt Hall, 1870 Miner Circle, Rolla, MO 65409-0410, U.S.A., e-mail: jhogan@umr.edu

## REGIONAL GEOLOGICAL SETTING

### *The southern Oklahoma aulacogen (SOA)*

The SOA formed as a result of intracontinental rifting during breakup of the Neoproterozoic supercontinent Pannotia in Late Proterozoic to Cambrian time (McConnell and Gilbert, 1990). Subsequent to Cambrian rifting, a large interior basin developed over the aulacogen and igneous rocks of the rifting event were buried by 4–5 km of Cambrian to Mississippian sediments (Gilbert, 1992). During the Ouachita Orogeny (late Mississippian to early Pennsylvanian time) igneous rocks of the SOA were uplifted as large horst blocks and then reburied by sediment derived locally and from the ancestral Ouachita Mountains. Subsequent erosion has exposed the volcanic and plutonic rocks that formed this rift such that locally the present erosional surface is not far below the level of the Cambrian surface (Fig. 1).

### *Igneous stratigraphy*

Bimodal igneous activity and tectonism accompanied formation of the SOA . The early phase of igneous activity was dominated by intrusion of a substantial volume of gabbroic magma, the Glen Mountains Layered Complex, with possible eruptive equivalents, the Navajoe Mountain Group. The later phase of igneous activity was dominated by voluminous felsic magmatism, including an extensive volcanic pile, the Carlton Rhyolite Group, and intrusion of large sheet-granites at the base of the rhyolite pile, such as the Mount Scott Granite. A period of substantial uplift and erosion, accentuated by normal faulting and extension of the brittle crust during rifting (McConnell and Gilbert, 1990), coincided with the hiatus separating early mafic and late felsic igneous activity (Ham *et al.*, 1964) such that the subaerial Carlton Rhyolite Group rests unconformably on the underlying Glen Mountains Layered Complex (Fig. 2).

Recent geochronological studies indicate a close temporal relationship for mafic and felsic magmatism

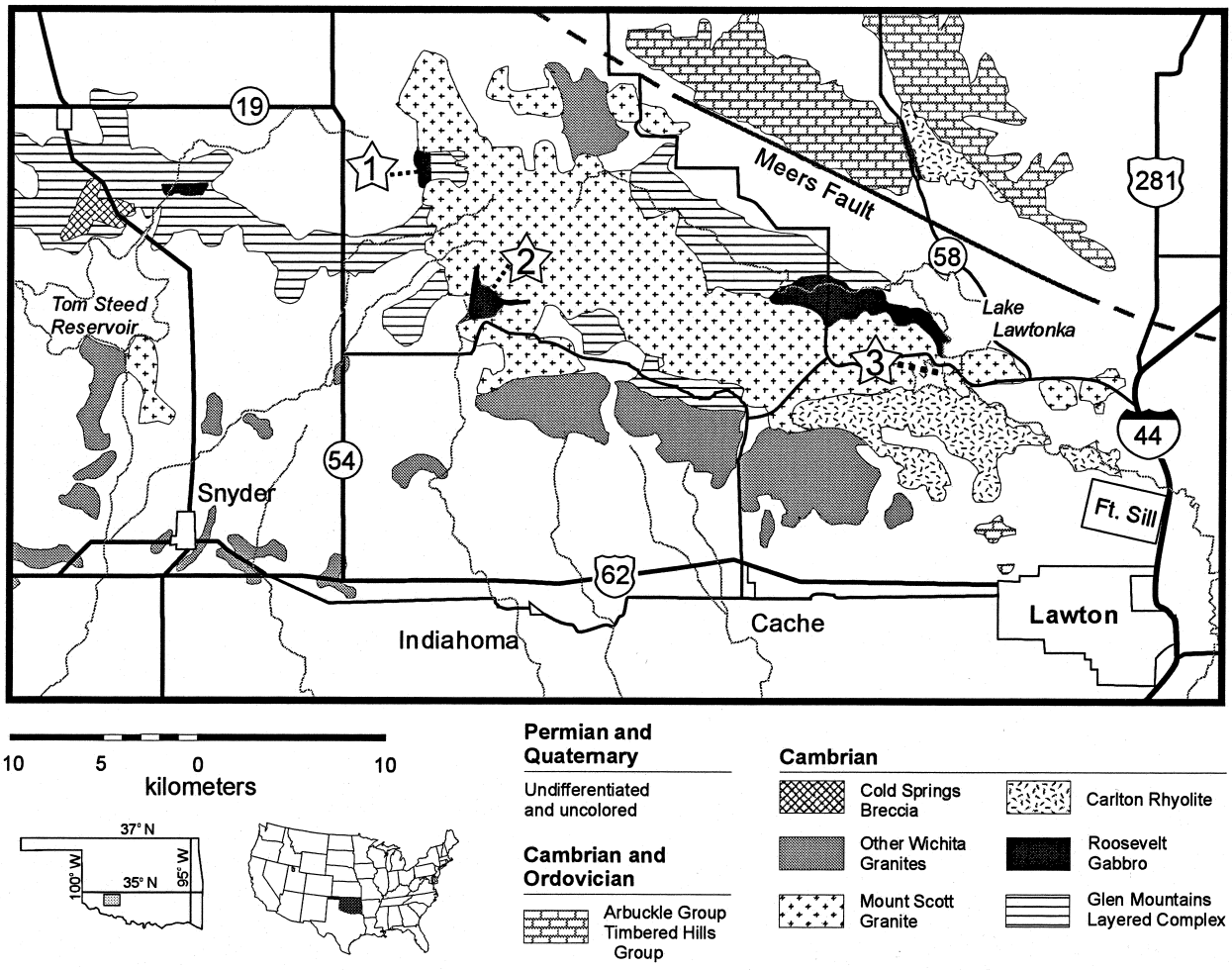


Fig. 1. Geological map of the eastern and east-central Wichita Mountains Igneous Province of southwestern Oklahoma, modified from Powell *et al.* (1980a, b). Numbered stars refer to locations discussed in the text: (1) Cut-throat Gap, (2) Sandy Creek member of the Roosevelt Gabbro, and (3) Elmer Thomas Lake dam.

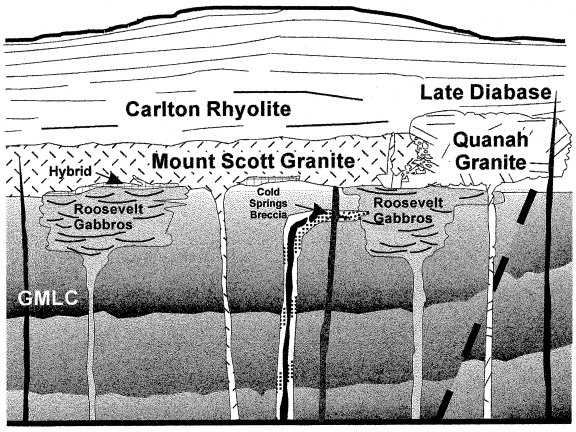


Fig. 2. Schematic cross-section showing the spatial relationships of *exposed* igneous rocks of the Wichita Mountains Igneous Province during Cambrian time. Felsic igneous units typically occur above and mafic igneous units below the Cambrian angular unconformity on the Glen Mountains Layered Complex (GMLC).

associated with the rifting event (Hogan *et al.*, 1996). A $^{40}Ar/^{39}Ar$ laser probe study of primary biotite and amphibole from the Mount Sheridan Gabbro recorded similar ages of $533 \pm 4$ which are younger than a $539 \pm 2$ Ma age for amphibole from the Mount Scott Granite sheet (Hames *et al.*, 1995). The close agreement between amphibole and biotite ages are consistent with rapid cooling of a shallow intrusive and are interpreted to represent the crystallization age of this pluton. Thus, biotite-bearing gabbro plutons of Roosevelt Gabbro are likely to be coeval with, or post-date, crystallization of the granite sheets (see Price *et al.*, in press). At the present erosional level, rock types owing their origin to magma mingling appear to be a minor component. The Late Diabase represents the last phase of igneous activity (Gilbert and Hughes, 1986).

### *Inferred Cambrian subsurface crustal structure*

Figure 3 is a Cambrian cross-section of the SOA reconstructed from geophysical and petrological arguments. A second, more substantial, mafic complex is postulated to reside at ≈15–21 km depth (Coffman *et al.*, 1986). Hogan and Gilbert (in press) infer this mid-crustal igneous complex to be akin to anorthosite–mangerite–charnockite–granite (AMCG) complexes. McConnell and Gilbert (1990) suggest extension of the middle crust was accommodated by emplacement of this complex, whereas extension of the upper crust was accommodated by normal faults that merged into a low angle master detachment fault rooted at the brittle–ductile transition (≈7–8 km depth). This depth also coincides with the buried Proterozoic basement–cover contact (Coffman *et al.*, 1986). Combined, these

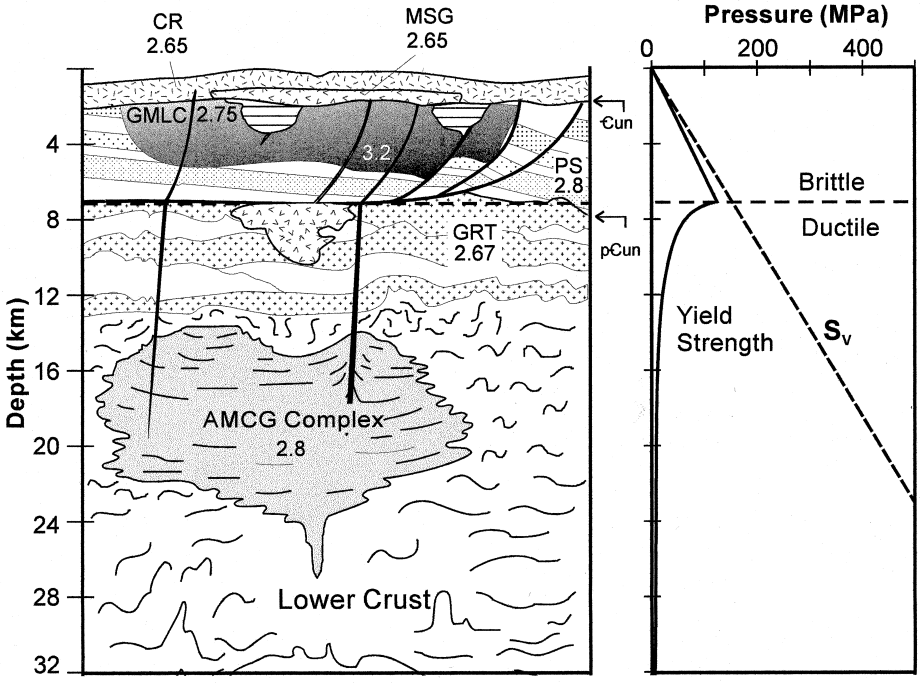


Fig. 3. Inferred Cambrian cross-section of the crust beneath the Southern Oklahoma Aulacogen in the vicinity of the Wichita Mountains, southwestern Oklahoma. Abbreviations of major units shown are as follows: CR = Carlton Rhyolite Group, MSG = Mount Scott Granite sheet, GMLC = Glen Mountains Layered Complex, PS = Proterozoic sediments, GRT = mid-Proterozoic Granite–Rhyolite Terrane, AMCG = Anorthosite–Mangerite–Charnockite–Granite Complex. Density of units (g cm$^{-3}$) are from Coffman *et al.* (1986). Roosevelt Gabbro plutons shown with horizontal rule, and Late Diabase dikes as black lines. The location of the early Cambrian unconformity is shown by €un and the unconformity between the Proterozoic cover and basement by p€un. Note that rift-related listric normal faults sole into the brittle–ductile transition which approximately coincides with the Proterozoic basement–cover contact. Variation in the yield strength of the crust and the vertical stress ($S_v$) as a function of depth during the Cambrian from Hogan and Gilbert (1995).

Table 1. Whole-rock compositions of igneous rocks

| Oxides | 1 | 2 | 3 | 4 | 5 | 6 | 7 | 8 | 9 |
|---|---|---|---|---|---|---|---|---|---|
| $SiO_2$ | 75.10 | 73.56 | 45.78 | 47.95 | 54.73 | 43.45 | 48.26 | 48.1 | 47.21 |
| $TiO_2$ | 0.22 | 0.45 | 1.36 | 2.88 | 2.83 | 5.67 | 0.94 | 1.57 | 3.76 |
| $Al_2O_3$ | 11.50 | 12.59 | 16.24 | 14.95 | 13.22 | 11.36 | 17.36 | 16.26 | 13.62 |
| $Fe_2O_3$* | 2.38 | 3.82 | 11.88 | 13.44 | 12.76 | 18.76 | 11.86 | 12.77 | 14.92 |
| MnO | 0.03 | 0.08 | 0.16 | 0.19 | 0.20 | 0.26 | 0.15 | 0.17 | 0.25 |
| MgO | 0.08 | 0.34 | 12.96 | 6.91 | 3.49 | 6.26 | 9.19 | 7.89 | 5.69 |
| CaO | 0.37 | 1.17 | 9.09 | 10.16 | 7.08 | 10.84 | 9.17 | 9.79 | 9.4 |
| $Na_2O$ | 4.05 | 3.73 | 2.03 | 2.6 | 3.51 | 2.19 | 2.54 | 2.56 | 2.54 |
| $K_2O$ | 4.32 | 4.30 | 0.30 | 0.58 | 1.64 | 0.33 | 0.46 | 0.58 | 0.79 |
| $P_2O_5$ | 0.02 | 0.08 | 0.18 | 0.34 | 0.54 | 0.90 | 0.17 | 0.2 | 0.6 |
| L.O.I. | 0.47 | | 0.44 | 0.73 | 0.12 | 0.03 | 0.01 | 0.13 | 1.24 |
| Total | 100.16 | 100.12 | 100.42 | 100.73 | 100.12 | 100.02 | 100.07 | 100.01 | 100.02 |

1. W792 Carlton Rhyolite, Wichita Mountains Wildlife Refuge, Oklahoma (Gilbert *et al*., 1990).
2. Average of six medium- to fine-grained, amphibole–biotite granites from the Mount Scott Granite, Oklahoma (Price *et al*., 1996a).
3. Average of nine High MgO gabbros, Sandy Creek Gabbro, Oklahoma (Diez de Medina, 1988).
4. Average of 13 Moderate MgO gabbros, Sandy Creek Gabbro, Oklahoma (Diez de Medina, 1988).
5. Low MgO gabbro, Sandy Creek Gabbro, Oklahoma (Diez de Medina, 1988).
6. Average of two High Ti gabbros, Sandy Creek Gabbro, Oklahoma (Diez de Medina, 1988).
7. Average of 29 high-Al biotite gabbro dikes, Greaser intrusion, Laramie Anorthosite Complex, Wyoming (Mitchell *et al*., 1995).
8. Average of 14 other high-Al biotite gabbro dikes, Laramie Anorthosite Complex Wyoming (Mitchell *et al*., 1995).
9. Average of 10 Late Diabase dikes, Southern Oklahoma Aulacogen (Aquilar, 1988).

$Fe_2O_3$* = total Fe as $Fe_2O_3$.
L.O.I. = loss on ignition

features form a significant subhorizontal anisotropy in the the crustal column.

## INTRUSION FORMS

Examples of the common forms which felsic and mafic magmas acquire at the emplacement level, as well as estimates of intensive parameters at the source depth and at the emplacement level, are presented.

### *Carlton Rhyolite Group*

The Carlton Rhyolite Group consists of a thick sequence (up to 1.4 km thick) of subaerial flows, minor ignimbrites, minor air-fall tuffs, agglomerates, and rare basalt flows (Ham *et al*., 1964). Although outcrops of Carlton Rhyolite are of limited extent (Fig. 1), subsurface drilling has documented the voluminous (44,000 $km^2$) nature of this unit (Ham *et al*., 1964). The presence of single, large flow-banded rhyolite (Bigger and Hanson, 1992) and the paucity of recognized air-fall tuffs (Ham *et al*., 1964) argue against an ash-fall origin to account for its widespread aerial extent.

Lavas of the Carlton Rhyolite Group are typically porphyritic, with phenocrysts of alkali-feldspar, lesser plagioclase, oxides, and variable amounts of embayed quartz, which can be locally absent, and pseudomorphs of a mafic silicate, presumably pyroxene (Ham *et al*., 1964). Zircon and apatite occur as accessory minerals. The groundmass is variably recrystallized and locally exhibits devitrification textures (Ham *et al*., 1964; Bigger and Hanson, 1992).

Carlton Rhyolite is typical of A-type igneous rocks. It has low CaO, high Fe/Fe + Mg, elevated abundances of high field strength elements (e.g. Zr $\approx$ 600–750 ppm), and distinctly within-plate trace element characteristics (Table 1) (Weaver and Gilbert, 1986). Zr geothermometry indicates crystallization temperatures of $\approx$950°C (Hogan and Gilbert, 1997) consistent with initial precipitation of vug-quartz as $\beta$-tridymite and $\beta$-cristobalite (Bigger and Hanson, 1992). These liquids are presumed to have orginated as high-temperature low-$H_2O$ partial melts from 12–15 km depth as a result of intrusion of the mid-crustal mafic complex (McConnell and Gilbert, 1990).

### *Mount Scott Granite sheet*

Members of the Wichita Granite Group, of which the Mount Scott Granite sheet is typical, form subhorizontal granite sheets preferentially localized along the unconformable contact between the underlying Glen Mountains Layered Complex and the overlying Carlton Rhyolite Group (Fig. 2). Stoped blocks of country rock are locally abundant along the lateral margins but rare within the interior and floors of these granite sheets. This dichotomy in intrusive style (i.e. uplifting the roof vs stoping the margins) may reflect variation in the local stress regime in the country rock around the intrusion (Hogan and Gilbert, 1997).

The Mount Scott Granite sheet, $\approx$55 km in length, $\approx$17 km wide, and a maximum thickness of $\approx$0.5 km, is the largest recognized individual sheet cropping out in the Wichita Mountains (Fig. 1). The basal contact of the Mount Scott Granite sheet with the underlying Glen Mountains Layered Complex is well defined in a regional sense. Local breaches in the granite cliffs (Fig. 4) provide erosional windows where the subhorizontal floor of the granite sheet can be readily seen to rest on anorthositic gabbro of the Glen Mountains

Fig. 4. Regional gabbro–granite relationships in the Wichita Mountains, Oklahoma, as viewed along the southern side of Cut-throat Gap. The Mount Scott Granite sheet forms barren rocky cliffs and overlies the vegetated slopes underlain by anorthositic gabbros of the Glen Mountains Layered Complex.

Layered Complex (Gilbert and Hogan, 1995). Although locally modified by intrusion of Roosevelt Gabbro (Price *et al.*, in press), the subhorizontal nature of the granite sheet is also discerned from regional map patterns (Hogan and Gilbert, 1997) (Fig. 1). Locally the roof of the Mount Scott Granite sheet can be traced to grade continuously into spherulitic rhyolite (Myers *et al.*, 1981). Such spatial relationships are consistent with subvolcanic emplacement of a relatively thin, sheet-like magma chamber.

Petrographic characteristics of Mount Scott Granite (Hogan and Gilbert, 1995, 1997; Price *et al.*, 1996a) are summarized here. It is predominantly a medium- to fine-grained, inequigranular, porphyritic, leucocratic alkali-feldspar granite. Early crystallizing ternary anorthoclase phenocrysts locally exhibit rapakivi texture and are set in a microgranitic to variably granophyric (0–>70 vol.%) groundmass. Ferro-edenitic hornblende, Fe-rich biotite, magnetite, and ilmenite are common minor phases. Accessory minerals include zircon, apatite, titanite, fluorite, ±allanite, and carbonate. Aplite dikes, pegmatite dikes, and miarolitic cavities are rare, and where present, signify an intrinsically low volatile content for this magma because very low emplacement pressures were needed to achieve saturation. Relatively low melt–$H_2O$ content (≈2 wt %) and high $F_2$ content (>1 wt%) for Mount Scott Granite are implied by experimental studies (Price *et al.*, 1996b). Considering evidence for local segregation of zircon at the emplacement level, and the apparent absence of inherited zircon (Wright *et al.*, 1996), temperatures of ≈900–950°C recorded by Zr and $P_2O_5$ geothermometry (Hogan and Gilbert, 1997) may represent minimum liquidus temperatures, consistent with early crystallization of ternary anorthoclase.

The rapakivi and porphyritic texture reflects a complicated crystallization history for Mount Scott Granite (Price *et al.*, 1996a). The magma originated by partial melting at ≈12–15 km depth under 'dry' conditions (McConnell and Gilbert, 1990) and underwent partial crystallization in a temporary storage chamber at 200 MPa (≈7.5 km depth), before being emplaced beneath the Carlton Rhyolite Group at a depth of 1.4 km or less (Hogan and Gilbert, 1995). Hogan and Gilbert (1995) noted that the bulk composition of the magma (excluding volatile components) apparently changed very little while traversing the crust, implying rapid ascent and approximation of closed-system equilibrium crystallization.

### *Sandy Creek Gabbro*

Small gabbro plutons (<20 $km^2$) and dikes of Roosevelt Gabbro, of which Sandy Creek Gabbro is typical, intrude the Glen Mountains Layered Complex (Fig. 1). The plutons are typically layered and internally differentiated, from olivine gabbro to Fe-rich quartz diorite and tonalite (Powell *et al.*, 1980a, b; Diez de Medina, 1988). Roosevelt Gabbros typically contain primary biotite and primary amphibole, in addition to plagioclase, two pyroxenes, ±olivine (Powell *et al.*, 1980a, b; Diez de Medina, 1988; Aquilar, 1988). Alkali feldspar and quartz occur in the more evolved rock types. Pegmatite occurs as dikes and pods and locally contains miarolitic cavities. The rock types become increasingly more felsic towards the contact with the overlying Mount Scott Granite. This contact is commonly obscured by talus, and where exposed is marked by the presence of an enigmatic, hybrid unit (Powell *et al.*, 1982). Thus, collection of fractionates roofward, as well as local assimilation of granite, may have been important processes during crystallization. Along with locally well-developed layering, this implies the majority of crystallization occurred at the emplacement level. Such features are consistent with crystallization of an intrinsically hydrous gabbroic magma at shallow crustal levels.

The Sandy Creek Gabbro is well exposed in an erosional window through the Mount Scott Granite sheet near Hale Spring (Fig. 1). The gabbro is spatially associated with the same unconformity that was the locus for intrusion of the Mount Scott Granite sheet (cf. Fig. 2). Xenoliths of Glen Mountains Layered

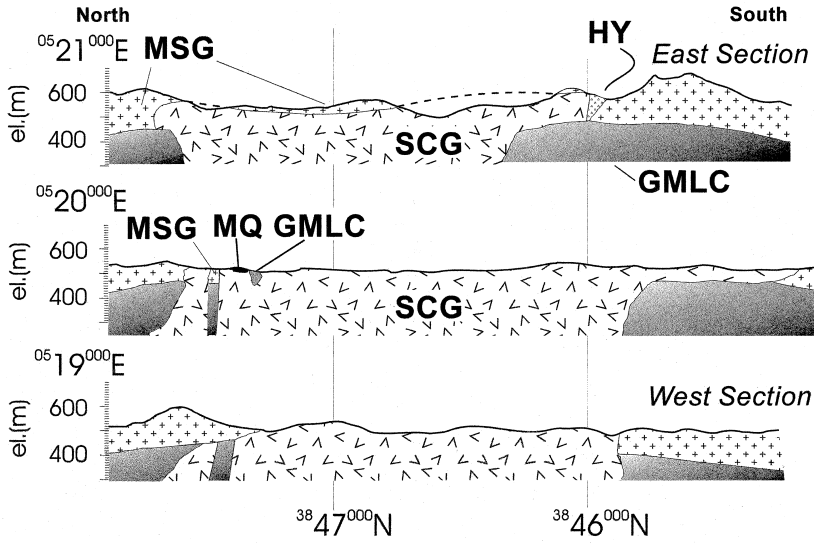


Fig. 5. Spatial relationships of the Sandy Creek Gabbro (SCG) with respect to the overlying Mount Scott Granite sheet (MSG), underlying Glen Mountains Layered Complex (GMLC), Meers Quartzite (MQ), and hybrid rock (HY). Dikes of Hale Spring Pegmatite not shown. Based on detailed field mapping, magnetometer surveying, and shallow drilling as described in Price *et al.* (in press). See text for discussion.

Complex and Meers Quartzite within the Sandy Creek Gabbro are spatially associated, consistent with the Meers Quartzite originating on an erosional surface on the Glen Mountains Layered Complex.

Price *et al.* (in press) modeled the spatial relationships between Sandy Creek Gabbro, Glen Mountains Layered Complex, and Mount Scott Granite through detailed mapping, magnetic surveying, and limited core drilling. The form of the Sandy Creek Gabbro is distinct from the Mount Scott Granite (Fig. 5). Rather than spreading out as a thin sheet along this contact, the Sandy Creek Gabbro is best viewed as a steep-sided oval cylinder, with short and long axes of approximately 1.5 km and 5.0 km, respectively, and a flat flared top. Only locally, and for a limited extent, does the gabbro form a thin tongue along the older unconformity and floor of the Mount Scott Granite. The gabbro is likely to have created space through a combination of stoping, partial melting of the roof rocks, and to a limited extent by lifting of the overburden (Price *et al.*, in press). Additional space may have been created through subsidence of the floor (Cruden, in press).

Hogan and Gilbert (in press) noted that whole rock compositions of Roosevelt Gabbro are broadly similar to high-Al biotite-gabbros from AMCG complexes (Table 1). Whole-rock compositions of Sandy Creek Gabbro, projected from Wollastonite on to the quartz–olivine–plagioclase plane (Longhi, 1991) plot in the vicinity of the 500–1150 MPa boundary lines and peritectics for liquids multiply saturated in olivine, plagioclase, and low-Ca pyroxene (Fram and Longhi, 1992), suggesting derivation of these liquids from a broad range of depths, from ≈15 to 35 km (Fig. 6). We suggest that this signature is consistent with temporary storage and equilibration of these mantle derived magmas in a mid-crustal mafic complex (Fig. 3) and previously at the base of the lithosphere. However, more direct comparisons are obscured by the cumulate nature of Roosevelt Gabbro samples.

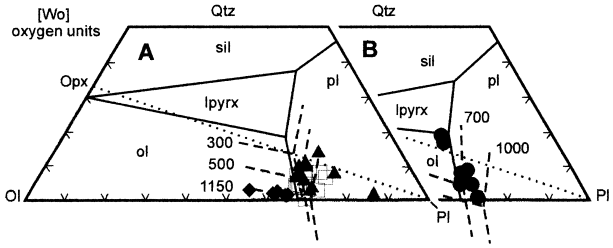


Fig. 6. Projection of whole-rock compositions of samples of the Sandy Creek Gabbro (A) and Late Diabase (B) from wollastonite [Wo] on to the olivine (Ol)–plagioclase (Pl)–silica (Qtz) plane following the method of Longhi (1991; personal communication, 1997). (A) Liquidus phase boundaries at 100 MPa (solid line) and 300, 500, and 1150 MPa (dashed lines) are those of Fram and Longhi (1992) for a high-Al gabbro composition typical for anorthosite–mangerite–charnockite–granite (AMCG) complexes. (B) Liquidus phase boundaries at 100 MPa (solid line) and 700 and 1000 MPa (dashed lines) are those of Vander Auwera and Longhi (1994) for a fine-grained jotunite from the Bjerkreim–Sokndal intrusion of the Rogaland Anorthosite–Mangerite–Charnockite–Granite (AMCG) Complex, Norway. Fields for silica polymorphs (sil), olivine (ol), plagioclase (pl) and low-Ca pyroxene (lpyrx) are also shown. Opx = orthopyroxene. (A) Bulk compositions of Sandy Creek Gabbro [shaded triangle = Moderate-MgO gabbro of the Mount Baker Rossevelt Gabbro; shaded diamond = High-MgO gabbro of the Sandy Creek Roosevelt Gabbro; open square = Moderate-MgO gabbro of the Sandy Creek Roosevelt Gabbro, data sources are Aquilar (1988) and Diez de Medina (1988)] coincide with boundary lines for liquids multiply saturated with olivine–low-Ca pyroxene–plagioclase at pressures between 500 and 1150 MPa. (B) Late Diabase bulk compositions define a linear trend that coincides with the trace of liquids multiply saturated with olivine–low-Ca pyroxene–plagioclase as a function of changing pressure. The majority of Late Diabase samples plot near the 700 MPa piercing point.

*Diabase dike at Elmer Thomas dam*

Numerous dikes of basaltic composition, 'Late Diabase' intrude nearly all other igneous rocks types, and thus represent the last phase of igneous activity associated with the rift (Gilbert and Hughes, 1986). The dikes are fine-grained and porphyritic. Plagioclase (labradorite) phenocrysts are set in a subophitic groundmass of labradorite, augite, ±hypersthene, ±magnetite, ±ilmenite. They have major-element compositions that are olivine- and nepheline-normative, and trace-element abundances transitional between tholeiite and alkaline magmas, with a distinct within-plate signature (Table 1) (Gilbert and Hughes, 1986; Cameron *et al.*, 1986). Their major-element compositions bear a close resemblance to the composition of ferrodiorite dikes, and are distinct from those of the high-Al biotite gabbro dikes, of AMCG complexes (Hogan and Gilbert, in press).

Gilbert and Hughes (1986) suggested Late Diabase originated from a mid-crustal (15–20 km depth) mafic complex inferred to lie within the SOA (cf. Fig. 3). Compositions of Late Diabase, plotted on the quartz–olivine–plagioclase plane (Longhi, 1991), along with the experimentally determined phase boundaries for a representative 'AMCG-ferrodiorite' (Vander Auwera and Longhi, 1994), form an elongated field that coincides with the trace of the composition of liquids saturated with olivine, plagioclase, and low-Ca pyroxene at various pressures (Fig. 6). This suggests equilibration of these magmas at different depths in the crust before their final intrusion as dikes in the near surface. However, the vast majority of the samples plot near the 700 MPa peritectic between olivine, low-Ca pyroxene, and plagioclase, consistent with these liquids originating from depths of between ≈20 and 25 km.

Field relationships of Late Diabase dikes cropping out at Lake Elmer Thomas dam (Gilbert *et al.*, 1990) are of particular significance to this study. The dikes are well exposed in an old quarry near the north side of the dam and are typical of Late Diabase from other localities in the Wichita Mountains. Here, several subparallel dikes, striking generally north, cross-cut Mount Scott Granite. All of the dikes exhibit well defined 'chill-margins' against Mount Scott Granite, but also locally partially melted the adjacent granite, implying a relatively high ambient temperature for Mount Scott Granite (>300°) at the time of dike intrusion (Price *et al.*, 1996c). More importantly, along the southern end of the exposure, erosion has stripped away Late Diabase, and the *bottom floor* of the dikes is observed (Fig. 7). At least locally, flow in these dikes must have been nearly horizontal, rather than vertical, as the dikes disappear both downwards and upwards. Thus, forces promoting and resisting magma ascent were approximately balanced at the depth of emplacement.

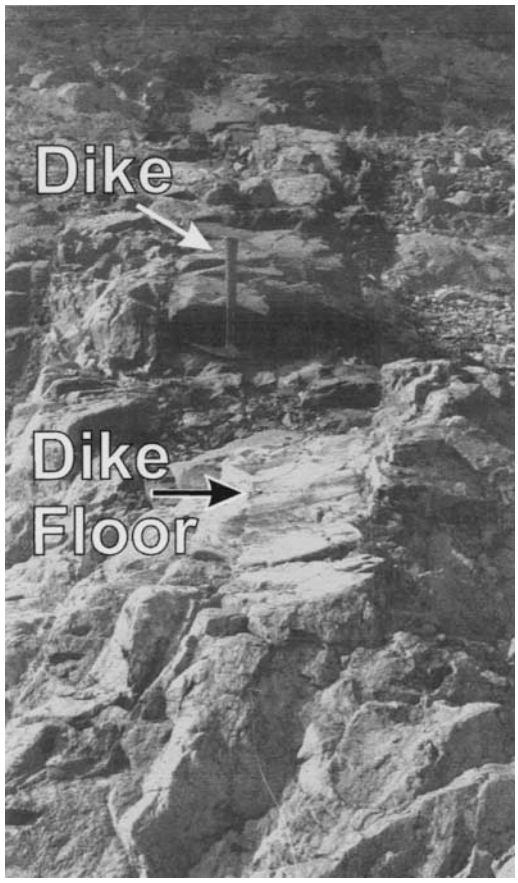


Fig. 7. Late Diabase dike at Elmer Thomas dam, Wichita Wildlife Refuge, Oklahoma. Here a steeply dipping (approximately 85°) diabase dike cross-cuts Mount Scott Granite. The diabase dike erodes faster than the Mount Scott Granite, and in the foreground has been completely eroded away exposing the floor of the dike, which is a relatively smooth surface of hornfelsed Mount Scott Granite. Here, this dike was propagating laterally rather than vertically.

## MAGMASTATIC ANALYSIS

Magma transport is greatly facilitated by fractures (Clemens and Mawer, 1992). Two types of magma transport within fractures are recognized (Nakashima, 1993): (1) transport within fractures that become isolated from the magma reservoir, (2) transport within fractures that maintain connectivity with the magma reservoir. The ascent of isolated liquid-filled cracks is driven by the buoyancy of the liquid with respect to its immediate surroundings, and such magma-filled cracks may rise to the level of neutral buoyancy, or alternatively, terminate against a subhorizontal mechanical anisotropy (Weertman, 1971, 1980). Magma ascent within a fracture (i.e. dike) that remains connected to a magma reservoir is driven by the magma driving pressure (Baer and Reches, 1991). In a homogeneous crust, magma within fractures that remain connected to the reservoir has the potential to ascend to the level in the crust where the magma driving pressure becomes negligible. In a heterogeneous crust, large-scale horizontal anisotropies (e.g. the brittle–ductile transition) can trap rising magma at deeper crustal

levels under the conditions that the magma driving pressure exceeds the lithostatic load at the depth of the anisotropy (Hogan and Gilbert, 1995).

Throughout Earth history, voluminous quantities of dense Fe-rich tholeiitic liquids have risen through continental crust of *lesser* density and spilled out on to the surface as flood basalts. These magmas rose through the continental crust despite their 'negative' buoyancy. Their presence implies large volumes of magma are transported within dikes that maintain connectivity with the underlying magma reservoir. Assuming this mode for magma transport, then the level at which rising magma stops (i.e. the emplacement level) and acquires its final shape, is to an extent determined by the magma driving pressure. The relationship between magma driving pressure, level of emplacement, and final form of igneous intrusions in an extensional tectonic setting will be explored using intrusions from the Wichita Mountains Igneous Province as examples.

## *Magma driving pressure*

The magma driving pressure ($P_d$) is the difference between the sum of the forces that support dike propagation and the remote compressive stress perpendicular to the dike wall (Baer and Reches, 1991). $P_d$ can be represented by

$$P_d = P_h + P_o - P_{vis} - S_h \quad (1)$$

where $P_h$ is the hydrostatic pressure, $P_o$ is the magma chamber overpressure, $P_{vis}$ is the viscous pressure drop, and $S_h$ is the tectonic stress perpendicular to the dike wall. The convention that compressive stresses are positive is adopted here.

*Hydrostatic pressure ($P_h$).* The hydrostatic pressure is the difference between the lithostatic pressure on the top of the magma reservoir, at a source depth $D$, and the pressure at the tip of the column of magma, at some depth $Z$, as it rises through the crust. The hydrostatic pressure as a function of depth $[P_h]_Z$ can be represented by

$$[P_h]_Z = \rho_c g D - \rho_m g (D - Z) \quad (2)$$

where $\rho_c$ is the integrated density of the crustal column, $\rho_m$ the integrated density of the magma, and $g$ the acceleration due to gravity.

Values for the density of the crust as a function of depth $[\rho_c]_Z$ are shown in Fig. 3. Magma density, as a function of temperature, pressure, and composition were estimated from measured whole-rock compositions (Table 1) following the method of Bottinga and Weill (1970) and using the partial molar volumes, thermal expansions, and compressibilities of oxide components of Lange and Carmichael (1990) and Toplis *et al.* (1994). The $Fe^{2+}/Fe^{3+}$ of the liquids, as a function of temperature and pressure, at an oxygen fugacity defined by the assemblage fayalite + magnetite + $\beta$-quartz (Frost, 1991), were estimated using the expression of Kress and Carmichael (1991) and the compositions of the proposed liquids adjusted accordingly prior to density calculations. Magma densities for Sandy Creek Gabbro and Mount Scott Granite were calculated both 'dry' and assuming initial $H_2O$ contents of 0.5 wt% and 1.0 wt%, respectively. Densities for Carlton Rhyolite and Late Diabase were calculated assuming an initial $H_2O$ content of 1.0 wt% and 0.0 wt%, respectively. Densities for the various liquids, from 0 to 1000 MPa, were calculated at 100 MPa intervals, over a temperature range appropriate for

Table 2. Melt characteristics for magmastatic calculations

| 1 | 2 | 3 | | 4 | 5 | 6 | 7 | | | 8 |
|---|---|---|---|---|---|---|---|---|---|---|
| Unit | Source depth (km) | Liquidus $T$ (°C) | | $dT/dP$ (°C/MPa) | $H_2O$ content (wt %) | $Fe_2O_3/FeO$* | $\rho^{\dagger}$ $\rho = m{*}P$ (MPa) + $c$ | | | $P_{vis}^{\ddagger}$ (MPa km$^{-1}$) |
| | | 0.0 MPa | 1000 MPa | | | | $m$ | $c$ | $r^2$ | |
| Carlton Rhyolite | 15 | 950 | 1000 | 0.005 | 1.0 | 0.0487 | 1.70E-05 | 2.2873 | 1.000 | 0.5 |
| Mount Scott Granite | 8 | 900 | 950 | 0.005 | 0.0 | 0.0481 | 1.80E-05 | 2.3787 | 1.000 | 0.5 |
| Mount Scott Granite | 8 | 900 | 950 | 0.005 | 1.0 | 0.0481 | 1.71E-05 | 2.3264 | 1.000 | 0.5 |
| Sandy Creek Gabbro | 18 & 25 | 1225 | 1285 | 0.006 | 0.0 | 0.0422 | 1.41E-05 | 2.6885 | 1.000 | 0.5 |
| Sandy Creek Gabbro | 18 & 25 | 1225 | 1285 | 0.006 | 0.5 | 0.0422 | 1.37E-05 | 2.6561 | 0.998 | 0.5 |
| Late Diabase | 18 & 25 | 1140 | 1180 | 0.004 | 0.0 | 0.0415 | 1.56E-05 | 2.7245 | 1.000 | 0.5 & 0.75 |

* Calculated following the method of Kress and Carmichael (1991) at $T$, $P$, and $fO_2$ = fayalite + magnetite + ß-quartz (Frost, 1991). Values reported in this table are those for 0.0 MPa and the liquidus $T$ (°C) at 0.0 MPa.

† Values for melt density, calculated at $T$, $P$, $X_i$, (including adjustments in $Fe_2O_3/FeO$ at an $fO_2$ = fayalite + magnetite + ß-quartz, see column 7 of this table), following the method of Bottinga and Weill (1970), and using the partial molar volumes, thermal expansions and compressibilities of the oxide components of Lange and Carmichael (1990) and Toplis *et al.* (1994), over the range of liquidus temperatures and pressures as given in columns 3, 4, and 5 of this table, were linearly regressed to determine the coefficients for the slope ($m$), $y$-intercept ($c$) and the sum of the residuals squared ($r^2$) for these correlations.

‡ Values chosen for $P_{vis}$ are based on the work of Baer and Reches (1991) and are discussed in the text

their liquidus temperatures, assuming a change in temperature during ascent of 4–6°C per 100 MPa. These values were linearly regressed and the resulting expression was used to calculate the integrated magma density of the dike as a function of depth (Table 2)

$$\rho_m = ([\rho_m]_D + [\rho_m]_Z)/2 \quad (3)$$

for use in equation (2). The magmas were assumed to remain entirely liquid. This is a reasonable assumption considering the low phenocryst contents of Carlton Rhyolite, Mount Scott Granite and Late Diabase, and as previously discussed, the well-developed layering typical of Roosevelt Gabbro suggests these magmas also underwent the bulk of crystallization at the emplacement level.

*Overpressure of the magma chamber* ($P_o$). Overpressure is the amount by which pressure within the magma chamber exceeds the confining pressure and is typically generated by the tremendous volume increase associated with bubble nucleation for melts that reach vapor saturation. The contribution of overpressure to ascent for any of these magmas is considered negligible due to their intrinsically low volatile contents.

*Viscous pressure drop* ($P_{vis}$). This variable measures the viscous resistance to magma flow within a dike. Baer and Reches (1991) used a high value of 0.75 MPa $km^{-1}$ to model the viscous pressure drop for granitic magma. Values ranging from 0.1 to 0.75 MPa $km^{-1}$ are adopted here, as the relatively high fluorine contents for the felsic melts may have significantly reduced the viscosity of these magmas (Price *et al.*, 1996a, b).

*Horizontal stress* ($S_h$). The horizontal normal stress acting on the crust $S_h$ is composed of the sum of the lithostatic stress and the tectonic stress. The lithostatic stress is equal to the vertical stress $S_v$ and can be represented by

$$S_v = \rho_c g Z. \quad (4)$$

The tectonic stress is a function of the regional state of stress for the crust. During Cambrian rifting the regional stress state of the crust within the SOA was approximately at its tensile strength (McConnell and Gilbert, 1990). The tensile strength of the lithosphere at any given depth is defined by the lesser of the brittle yield strength and the ductile yield strength, and this strength as a function of depth gives a yield stress profile for the lithosphere (Lynch and Morgan, 1987). Following the method of Lynch and Morgan (1987), Hogan and Gilbert (1995) calculated a Cambrian yield strength profile for the crust within the SOA (Fig. 4). Variation in the horizontal normal stress as a function of depth $[S_h]_Z$ is calculated by subtraction of the yield strength profile of the crust from the lithostatic stress. Values for $[S_h]_Z$ calculated by Hogan and Gilbert (1995, Fig. 7) are adopted here.

The $P_d$ for each unit assuming a lithostatic state of stress for the crust

$$\sigma_1 = \sigma_2 = \sigma_3 = \rho_c g Z \quad (5)$$

can be calculated by substitution of (5) for $S_h$ in equation (1) and thus represents a $P_d$ devoid of influence from far-field regional tectonic forces. We utilize this particular magma driving pressure as a reference state '$P_m$' for comparitive purposes. For this stress regime, ignoring the minor role of $P_o$ and $P_{vis}$, the level to which magma may rise in a homogeneous crust is determined by the level of neutral buoyancy (i.e. the level at which $\rho_m = \rho_c$).

## RESULTS OF MAGMASTATIC CALCULATIONS

### *Carlton Rhyolite*

Variation in $[P_d]_Z$ for Carlton Rhyolite is plotted in Fig. 8. Ascending from a source depth of 15 km, $P_d$ for Carlton Rhyolite reaches a maximum value at the depth of the brittle–ductile transition and retains a large positive value of ≈60 MPa at the surface. $P_m$ for Carlton Rhyolite steadily increases with decreasing depth as $\rho_m$ is considerably less than $\rho_c$ and is equivalent to $P_d$ at the surface as $S_v$ goes to 0. Slight inflections in $P_d$ reflect local variation in crustal density. The large positive $P_d$ at the surface signifies the poten-

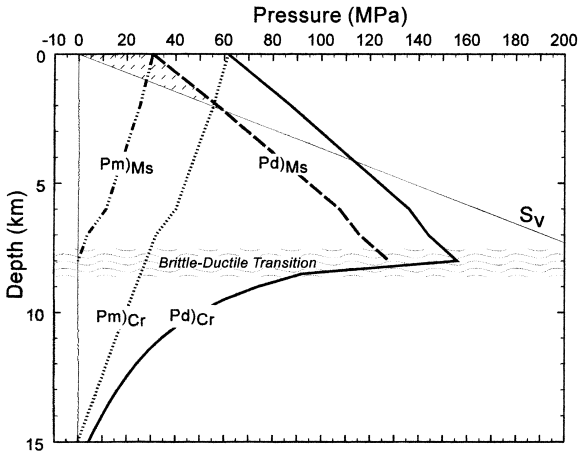


Fig. 8. Variation in the vertical stress ($S_v$), magma driving pressure ($P_d$), and magma pressure ($P_m$) of Carlton Rhyolite and Mount Scott Granite magma as a function of depth. Carlton Rhyolite magma, sourced from a reservoir chamber at a depth of 15 km, maintains a large positive $(P_d)_{CR}$ at the surface indicating the potential to erupt as rhyolite, and it did. Mount Scott Granite magma, sourced from a temporary storage chamber at ≈ 8 km depth maintains a large positive $(P_d)_{MS}$ at the surface also indicating a potential to erupt. In contrast, it did not. The presence of a subhorizontal anistropy in the crust (i.e. the unconformity at the base of the Carlton Rhyolite Group) at a depth where $(P_d)_{MS} > S_v$ (hachured region) acted as a CMT trapping the rising magma to crystallize as the Mount Scott Granite sheet. Positive values for both $(P_m)_{CR}$ and $(P_m)_{MS}$ throughout the crustal column indicate the potential for both magmas to escape the source region and erupt in a neutral regional stress regime (i.e. $\sigma_1 = \sigma_2 = \sigma_3 = \rho_c g Z$). However, for the Mount Scott Granite to have crystallized as an extensive subhorizontal sheet under such conditions the Carlton Rhyolite Group would have had to have been substantially less than 1 km thick.

tial for these liquids to rise through the entire crustal column and breach the surface. Considering the voluminous nature of the Carlton Rhyolite Group, many of these felsic liquids did just that.

*Mount Scott Granite sheet*

$P_d$ for Mount Scott Granite magma originating from a temporary storage chamber (≈8 km) steadily decreases with decreasing depth reaching a value of ≈30 MPa at the surface (Fig. 8). The difference in surface $P_d$ and $P_m$ for Mount Scott and Carlton Rhyolite principally reflects the difference in source depths for these two magmas. Before reaching the surface, $P_d$ and $P_m$ exceed $S_v$ at ≈2 km and 1 km depth, respectively.

Mount Scott Granite magma clearly had the potential to erupt and add to the rhyolite pile. However, it was emplaced as a thin, but expansive, sheet-granite along the unconformity between the overlying Carlton Rhyolite Group and the underlying Glen Mountains Layered Complex. The depth to this unconformity, as approximated by the thickness of the Carlton Rhyolite Group, probably did not greatly exceed 1.4 km (Fig. 4). This unconformity met the necessary conditions of a crustal magma trap: $P_d$ greatly exceeded $S_v$ at the depth of the anisotropy (Hogan and Gilbert, 1995). Thus, the magma had sufficent force to lift the overburden and spread out along the unconformity thereby terminating further ascent. Only if the rhyolite pile was significantly thinner than 1 km would the magnitude of $P_m$ have been sufficent to achieve the same result.

*Sandy Creek Biotite Gabbro*

In order to minimize the effects of crystal accumulation, the average bulk composition of high-Al biotite–gabbro dikes from the Laramie Anorthosite Complex (Mitchell *et al.*, 1995), with the addition of 0.5 wt% $H_2O$, was used as a proxy for the liquid composition that presumably gave rise to Sandy Creek Gabbro (Table 1). Variation in $[P_d]_Z$ and in $[P_m]_Z$ for such a magma is presented in Fig. 9. Source depths were chosen to coincide with the depth of the mid-crustal mafic complex at ≈16–25 km below the Cambrian surface (cf. Fig. 4). The difference in $P_d$ for a magma sourced from a reservoir at 18 km and at 25 km is negligible. Therefore, only $P_d$ and $P_m$ for a dike originating from a magma chamber at 25 km is shown. $P_d$ reaches a maximum at the brittle–ductile transition, and maintains a positive $P_d$ of ≈15 MPa at the surface. $P_d$ exceeds $S_v$ at ≈1.4 km depth and $P_m$ at ≈0.5 km. The positive $P_d$ at the surface indicates a potential for the eruption of mafic lavas may have existed. However, as previously discussed, intrusion of Sandy Creek Gabbro was localized along the same unconformity as intrusion of Mount Scott Granite, and the relatively flat roof of the Sandy Creek Gabbro

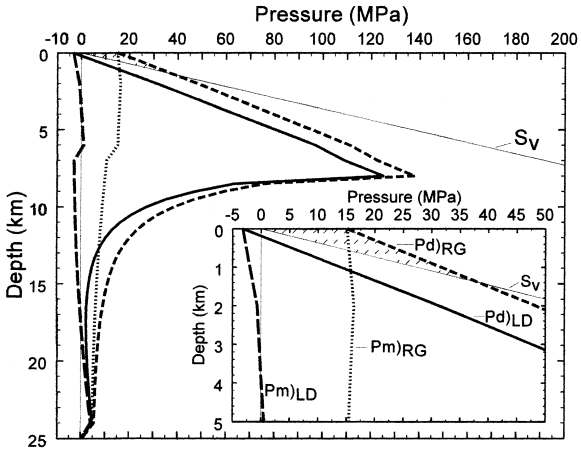


Fig. 9. Variation in the vertical stress ($S_v$), magma driving pressure ($P_d$), and magma pressure ($P_m$) for Sandy Creek Gabbro (RG) and for Late Diabase (LD) magma as a function of depth. Late Diabase magma, sourced from 25 km depth, has the potential to rise to ≈ 0.2 km from the surface at which point $(P_d)_{LD}$ becomes negligible. Negative values for $(P_d)_{LD}$ at the surface suggests that it is unlikely Late Diabase magma would have erupted as basalt. Furthermore, low to negative values for $(P_m)_{LD}$ indicate that it is highly unlikely Late Diabase would have been able to leave the source region *unless* the crust was being extended. Sandy Creek Gabbro magma, sourced from 25 km depth, maintains a positive $(P_d)_{RG}$ at the surface indicating the potential to erupt. However, biotite- or amphibole-bearing lavas have yet to be reported from the SOA. The presence of a sub-horizontal anistropy in the crust (i.e. the unconformity at the base of the Carlton Rhyolite Group now modified by intrusion of Mount Scott Granite) at a depth where $(P_d)_{RG} \cong S_v$ formed a CMT that trapped the rising magma, resulting in crystallization of the Sandy Creek Gabbro pluton. In contrast, $(P_m)_{RG} \geq S_v$ at depths less than 0.5 km suggesting that this CMT will be ineffective in stopping further rise of these magmas in subvertical dikes.

abuts against the base of the Mount Scott Granite sheet (Fig. 5). The presence of the additional thickness of the Mount Scott Granite sheet would have increased the depth to the unconformity probably no more than an additional 0.5 km. The $P_d$ for the rising mafic liquid may have approximated, but is unlikely to have greatly exceeded, $S_v$ at the depth of the unconformity or the depth of the base of the Mount Scott Granite sheet (≈2.0 km). Apparently, this $P_d$ was sufficient to activate this crustal magma trap and terminate further ascent of these magmas. In contrast, the considerably lower magnitude for $P_m$ at this depth suggests that, under such conditions, dikes containing these magmas would have continued their upward ascent having insufficent driving pressure to activate the crustal magma trap.

*Late Diabase dikes*

Variation in $[P_d]_Z$ and in $[P_m]_Z$ for Late Diabase is shown in Fig. 9. The source depth for these liquids, as previously discussed, is interpreted to coincide with the mid-crustal mafic complex at 16–25 km depth. Again the difference in source depth had negligible effect on the $P_d$ and only the curve for a dike originating from a magma reservoir at 25 km is shown.

Late Diabase maintains a positive $P_d$ until $\geqslant$0.2 km depth and at depths less than this becomes negative, reaching a value of $\approx -2$ MPa at the surface. In contrast, at depths less than 15 km the magnitude of $P_m$ is essentially less than or equal to zero, suggesting that Late Diabase magma is likely to remain trapped in the middle crust under such conditions (i.e. $\sigma_3 \geqslant \rho_c g Z$). The role of the regional stress in determining the viability of magma ascent and intrusion form is clear: as the density contrast between crust and magma diminishes, magma ascent becomes increasingly more unlikely, unless the crust is being sufficiently extended.

The $P_d$ for Late Diabase remains less than $S_v$ over the entire ascent through the crust (Fig. 9). This low, but positive, $P_d$ renders any subhorizontal anistropy ineffective as a crustal magma trap for Late Diabase. Thus, rising Late Diabase magma has the potential to ascend to the level at which the $P_d$ becomes negligible. For the relatively dense Fe-rich tholeiitic magmas that form the Late Diabase dikes in the Wichita Mountains, this depth was $\approx$0.2 km below the surface. The field relationships which locally demonstrate horizontal flow, rather than continued ascent, for the Late Diabase dike discussed earlier indicates the $P_d$ within this dike was low to negligible during intrusion. These calculations imply that less than 1 km of Mount Scott Granite and Carlton Rhyolite overlay this area at the time of dike intrusion. In addition, the negative $P_d$ calculated for these basaltic liquids at the surface may help to explain the relatively common occurrence of Late Diabase dikes throughout the SOA (e.g. Gilbert and Hughes, 1986; Denison, 1995) but the paucity of basaltic lavas recognized within the overlying volcanic cover (e.g. Ham *et al.*, 1964).

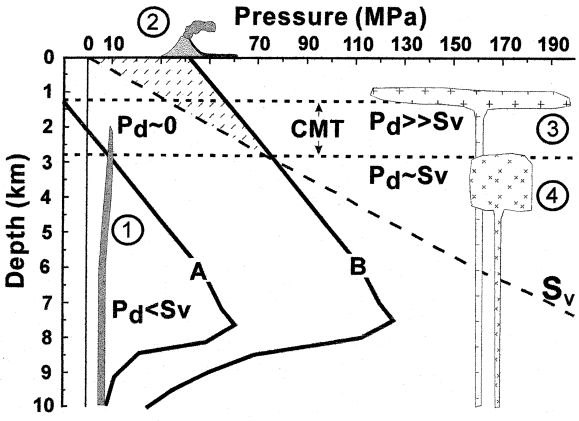


Fig. 10. Four hypothetical cases illustrating the role of magma driving pressure ($P_d$), vertical stress ($S_v$), and crustal magma traps (*CMT*) in determing the depth at which rising magma stops and the shape the pluton assumes. (1) Rising magma has the potential to continue its ascent through homogeneous crust to a depth where $P_d$ becomes negligible. For $(P_d)_A$ this depth is approximately 2 km and because $P_d < S_v$ at the emplacement level the magma will crystallize as a subvertical sheet (i.e. dike) oriented perpendicular to the direction of the least principal stress. (2) In contrast, magma that maintains a large positive $P_d$ at the surface, such as $(P_d)_B$, has the potential to erupt. However, the presence of a subhorizontal strength anisotropy in the crustal column (e.g. unconformity, brittle–ductile transition, etc.) can act as CMT, terminating magma ascent at a deeper crustal level, if $P_d \geq S_v$ (hachured region) at the depth of the anisotropy. The final form of the pluton, to an extent, is dependent on the magnitude of $P_d$ relative to $S_v$ at the depth of the CMT: (3) $(P_d)_B \gg S_v$ and the magma has sufficent $P_d$ to lift the overburden and spread out along the CMT to crystallize as a subhorizontal sheet. (4) $(P_d)_B \cong S_v$ and although the ascending magma will be trapped by the CMT, it has insufficient $P_d$ to lift the overburden and crystallizes as a steep-sided, relatively flat-topped, stock or batholith.

## DISCUSSION

The crustal level at which rising magma stops, and the final form it assumes, is to an extent a function of the magnitude of the $P_d$, the presence of subhorizontal anisotropies (e.g. unconformities, brittle–ductile transition), and the magnitude of the $S_v$ (i.e. lithostatic load) during ascent. The relationship among these variables is discussed in the following section.

### *Magma driving pressure, crustal magma traps, emplacement depth, and pluton shape*

Many factors, thermal (e.g. rates of heat loss), compositional (e.g. $H_2O$ content), and mechanical (e.g. horizontal planes of weakness) contribute to determining the potential crustal level to which magma can rise before solidifying (Hogan and Gilbert, 1995, 1997, and references therein). For viable ascent rates (i.e. those rapid enough to minimize the effects of heat loss), the concept of $P_d$ embodies many of these factors and allows assessment of compositional and mechanical factors in determining the emplacement level of an intrusion. Similarly, the final shape assumed by an intrusion, to a large extent, may be determined by the magnitude of $P_d$ relative to the $S_v$ and by the presence or absence of potential crustal magma traps. Two schematic $P_d$ curves, typical for igneous rocks of the SOA, illustrate the relationship between $P_d$, level of emplacement, and shape of plutons (Fig. 10). These relationships had a pronounced effect on determining the compositional structure of the Wichita Mountains.

*Curve A*. The magnitude of the $P_d$ represented by curve A is always less than the $S_v$ and becomes negative at depths less than 2.0 km (Region 1 in Fig. 10). A magma with this $P_d$ has the potential to ascend to within 2.0 km of the surface. At this depth further ascent is precluded by the negligible $P_d$ within the dike and here it may crystallize under the condition $P_d < S_v$ thus maintaining the form of a subvertical sheet or dike. This level has been referred to as the 'level of neutral buoyancy', a phrase that implies this singular force governs magma ascent, leading to the concept that the more felsic upper continental crust can act as a 'density filter', allowing the continued upward passage of buoyant felsic liquids while preventing the further rise of denser mafic liquids (e.g. Trønnes and Brandon, 1992). The common occurrence throughout Earth history of voluminous Fe-rich continental

tholeiites testifies to the fallacy of this idea. We prefer the concept of $P_d$ in order to emphasize that the magnitude of the density contrast between the object and its immediate surroundings (i.e. buoyancy) is but one of several factors that determines the potential level to which magma can rise in the crust. Thus, the ascending magma which formed the Late Diabase dikes within Mount Scott Granite at Lake Elmer Thomas dam arrested at a level in the crust where $P_d$ became negligible, and clearly could not have reached this depth without the contribution to $P_d$ from the regional state of stress of the crust (cf. Figure 9).

*Curve B*. The $[P_d]_Z$ represented by curve B exceeds the $S_v$ at $\approx$3 km depth and maintains a large positive value of $\approx$40 MPa at the surface. Barring the presence of crustal magma traps, a magma that maintains positive $P_d$ at the surface has the potential to erupt (Region 2 in Fig. 10). This was the case for A-type rhyolite flows of the Carlton Rhyolite Group. The intrinsically low $H_2O$ contents, potentially high fluorine contents, and large positive $P_d$ at the surface for these magmas favored their eruption in relatively non-explosive manner as flows of considerable aerial extent. However, the presence of a subhorizontal strength anisotropy in the crust, such as an unconformity, can potentially impede or terminate further ascent of a magma with such characteristics. To be an effective crustal magma trap $P_d$ must equal or exceed $S_v$ at the depth of the anisotropy (Hogan and Gilbert, 1995). For curve B, the presence of a crustal strength anisotropy within the hachured region on Fig. 10 satisfies these conditions (e.g. Regions 3 and 4 in Fig. 10). Rising magma trapped along such an anisotropy would solidify into a plutonic rock. For example, only subtle compositional differences exist between Carlton Rhyolite and Mount Scott Granite, suggesting both magmas had nearly equivalent potential to reach the surface and crystallize as rhyolite. Why is there a Mount Scott Granite? Eruption of rhyolite buried the unconformity to create a crustal strength anisotropy. This anisotropy was an effective crustal magma trap for subsequent rising felsic magmas ($P_d \geq S_v$ at this depth), thus localizing their intrusion along the buried unconformity where they spread out to solidify as granite sheets (Hogan and Gilbert, 1995, 1997).

The final shape assumed by an intrusion, to a large extent, may be determined by the magnitude of the $P_d$ relative to the $S_v$, and by the presence or absence of potential crustal magma traps. Many authors have suggested that subhorizontal sheet-like magma chambers can readily propagate, at low positive $P_d$, by splitting the host rock along a pre-existing discontinuity and lifting the roof (e.g. Chamberlin and Link, 1927; Anderson, 1951; Pollard, 1973; Weertman, 1980). We emphasize that the $P_d$ must *greatly exceed* the $S_v$ at the depth of the anisotropy if the magma is to have sufficient force to lift the overburden as a means of creating space. Such magmas can spread laterally along the discontinuity to crystallize as subhorizontal sheets (Region 3 in Fig. 10). The angular unconformity separating the Carlton Rhyolite Group and the Glen Mountains Layered Complex forms such a crustal magma trap for later rising felsic liquids that crystallized as A-type sheet granites of the Wichita Granite Group (Hogan and Gilbert, 1997). Similar emplacement conditions may have influenced the final form of the A-type sheet granites of the Bushveld Complex, South Africa (cf. Kleeman and Twist, 1989). In the case of the Wichita Granite Group, the extensive sheet forms were probably enhanced by the geometry of the feeder conduits (e.g. en échelon fractures) and by reduced magma viscosities as a result of intrinsically high melt fluorine contents (Hogan and Gilbert, 1997), as well as by large positive $P_d$ at the depth of the unconformity.

In contrast, if the magnitude of $P_d$ and $S_v$ are approximately equivalent at the depth of the crustal magma trap, further rise of the magma will be prevented, but the $P_d$ will be insufficient to lift the overburden. Thus, space will have to be created by other means (e.g. stoping) and the resulting pluton will be a thicker, more equant steep-sided stock (Region 4 in Fig. 10). Several Roosevelt Gabbro plutons crystallized with such forms along the same crustal magma trap that was previously exploited by Mount Scott Granite. The $P_d$ for rising mafic liquids was sufficient to activate this subhorizontal anisotropy as a crustal magma trap, but insufficient to substantially lift the overburden in order to create space for the intruding magma. Thus, rather than spreading out along the crustal magma trap to form an extensive sheet-like intrusion, the Sandy Creek Gabbro formed a steep-walled stock-like intrusion with a flat top that approximately coincides with the subhorizontal crustal magma trap. The presence of localized spreading along the subhorizontal crustal magma trap for the Sandy Creek Gabbro (Fig. 5) indicates at some time during the intrusion the $P_d$ probably exceeded the $S_v$. This could be achieved by decreasing $\rho_m$, by fluctuations in the regional stress regime (Hogan and Gilbert, 1995), or by influx of new magma into the reservoir chamber.

## CONCLUSIONS

The crustal level to which magma may rise and the final shape it assumes is to a large degree, not discounting many other factors (e.g. thermal history, feeder conduit shape), predetermined by the magnitude of the $P_d$ relative to the $S_v$, and by the presence of large-scale subhorizontal strength anisotropies that can act as crustal magma traps. In homogeneous crust, magma rising within a fracture that remains connected to the magma reservoir has the potential to ascend to the level at which the $P_d$ becomes negligible. Magma with a positive $P_d$ at the surface possesses the potential

to erupt. Rising magma may be trapped at deeper crustal levels by subhorizontal anisotropies present within the crustal column if the $P_d$ is greater than or equal to the $S_v$ at the depth of the anisotropy (i.e. crustal magma traps). Subhorizontal sheet-like intrusions form along these crustal magma traps when the $P_d$ greatly exceeds the $S_v$ at the depth of the trap. Under such conditions, the magma has sufficient $P_d$ to lift the overburden and allow the magma to spread laterally along the crustal magma trap prior to solidification. If the $P_d$ is approximately equivalent to the $S_v$ at the depth of the intrusion, magma ascent may be arrested, but the $P_d$ will be insufficient to lift the overburden. Under such conditions, the necessary space for the intrusion must be created by other processes (e.g. Cruden, 1998). The resulting pluton will have the form of a relatively thick, steep-sided stock or batholith, with possibly a flat roof. Finally, magma that solidifies at a depth where the $P_d$ is less than $S_v$ will have the form of subvertical sheets (i.e. dikes) oriented perpendicular to the direction of the least principal stress.

*Acknowledgements*—This work was supported in part by NSF grant ♯EAR-9316144 to J. P. Hogan and M. C. Gilbert, by a U.S.G.S. National Cooperative Mapping Program (EDMAP) grant contract ♯1434-HQ-96-AG-01547 to J. D. Price and M. C. Gilbert, and by Eberly Chair Funds available to M. C. Gilbert. This manuscript benefited from discussions with Z. Reches and L. Boldt and from reviews by S. Cruden, C. K. Mawer, and J. L. Vigneresse.

## REFERENCES

Anderson, E. M. (1951) *The Dynamics of Faulting and Dyke Formation With Applications to Britian*. Oliver and Boyd, Edinburgh.

Aquilar, J. (1988) *Geochemistry of mafic rock units of the Southern Oklahoma Aulacogen, southwestern Oklahoma*. Unpublished M.S. thesis, University of Oklahoma, Norman.

Baer, G. and Reches, Z. (1991) Mechanics of emplacement and tectonic implications of the Ramon dike systems, Israel. *Journal of Geophysical Research* **96,** 11,895–11,910.

Bates, R. L. and Jackson, J. A. (1980) *Glossary of Geology*. American Geological Institute, Falls Church, Virginia.

Bigger, S. E. and Hanson, R. E. (1992) Devitrification textures and related features in the Carlton Rhyolite in the Blue Creek Canyon area, Wichita Mountains, southwestern Oklahoma. *Oklahoma Geology Notes* **52,** 124–142.

Bottinga, Y. and Weill, D. F. (1970) Densities of liquid silicate systems calculated from partial molar volumes of oxide components. *American Journal of Science* **269,** 169–182.

Cameron, M., Weaver, B. L. and Diez de Medina, D. (1986) A preliminary report on trace-element geochemistry of mafic igneous rocks of the Southern Oklahoma Aulacogen. In *Petrology of the Cambrian Wichita Mountains Igneous Suite*, ed. M. C. Gilbert, pp. 80–85. Oklahoma Geological Survey Guidebook **23**.

Chamberlain, R. T. and Link, T. A. (1927) The theory of laterally spreading batholiths. *Journal of Geology* **35,** 319–357.

Clemens, J. D. and Mawer, C. K. (1992) Granitic magma transport by fracture propagation. *Tectonophysics* **204,** 339–360.

Coffman, J. D., Gilbert, M. C. and McConnell, D. A. (1986) An interpretation of the crustal structure of the Southern Oklahoma Aulacogen satisfying gravity data. In *Petrology of the Cambrian Wichita Mountains Igneous Suite*, ed. M. C. Gilbert, pp. 1–10. Oklahoma Geological Survey Guidebook, **23**.

Cruden, A. R. (1998) On the emplacement of tabular granites. *Journal of the Geological Society of London* **155,** 852–862.

Denison, R. E. (1995) Significance of air-photograph linears in the basement rocks of the Arbuckle Mountains. *Oklahoma Geological Survey Circular* **97,** 119–131.

Diez de Medina, D. M. (1988) *Geochemistry of the Sandy Creek Gabbro, Wichita Mountains, Oklahoma*. Unpublished M.S. thesis, University of Oklahoma, Norman.

Fram, M. S. and Longhi, J. (1992) Phase equilibria of dikes associated with Proterozoic anorthosite complexes. *American Mineralogist* **77,** 605–616.

Frost, B. R. (1991) Introduction to oxygen fugacity and its petrologic importance. In *Oxide Minerals: Petrologic and Magnetic Significance*, ed. D. H. Lindsley, pp. 1–9. Mineralogical Society of America, Reviews in Mineralogy, **25**.

Gilbert, M. C. (1992) Speculations on the origin of the Anadarko basin. In *Proceedings of the International Conference on Basement Tectonics*, ed. R. Mason, Vol. 7, pp. 195–208. Kluwer Academic, Boston.

Gilbert, M. C., Hogan, J. P. and Myers, J. D. (1990) Geology, geochemistry, and structure of low-pressure sheet granites, Wichita Mountains, Oklahoma. In *Guidebook for Field Trip no. 5: Geological Society of America Annual Meeting*.

Gilbert, M. C. and Hogan, J. P. (1995) Wichita Mountains Field Trip. In *Guidebook for the 12th International Conference on Basement Tectonics*. School of Geology and Geophysics, University of Oklahoma, Norman, Oklahoma.

Gilbert, M. C. and Hughes, S. S. (1986) Partial chemical characterization of Cambrian basaltic liquids of the Southern Oklahoma Aulacogen. In *Petrology of the Cambrian Wichita Mountains Igneous Suite*, ed. M. C. Gilbert, pp. 73–79. Oklahoma Geological Survey Guidebook, **23**.

Ham, W. E., Denison, R. E. and Merritt, C. A. (1964) Basement Rocks and Structural Evolution Southern Oklahoma. *Oklahoma Geological Survey Bulletin* **95,** 302.

Hames, W. E., Hogan, J. P. and Gilbert, M. C. (1995) Revised granite–gabbro age relationships, Southern Oklahoma Aulacogen. In *Abstracts from the 12th International Conference on Basement Tectonics*, Vol. 44. Norman, Oklahoma.

Hamilton, W. and Myers, W. B. (1974a) Nature of the Boulder Batholith of Montana. *Geological Society of America Bulletin* **85,** 365–378.

Hamilton, W. and Myers, W. B. (1974b) Nature of the Boulder Batholith of Montana: Reply. *Geological Society of America Bulletin* **85,** 1958–1960.

Hogan, J. P. and Gilbert, M. C. (1995) The A-type Mount Scott Granite Sheet: importance of crustal magma traps. *Journal of Geophysical Research* **100,** 15,779–15,793.

Hogan, J. P. and Gilbert, M. C. (1997) The intrusive style of A-type sheet granites from the Southern Oklahoma Aulacogen. In *Middle Proterozoic to Cambrian Rifting Mid-North America*, ed. R. W. Ojakangas, A. B. Dickas and J. C. Green, pp. 299–311. Geological Society of America Special Paper, **312**.

Hogan, J. P. and Gilbert, M. C. (1998) The Southern Oklahoma Aulacogen: A Cambrian analog for Mid-Proterozoic AMCG (Anorthosite–Mangerite–Charnockite–Granite) complexes. *Basement Tectonics*, **12** (in press).

Hogan, J. P., Gilbert, M. C., Price, J. D., Wright, J. E., Deggeller, M. and Hames, W. E. (1996) Magmatic evolution of the Southern Oklahoma Aulacogen. *Geological Society of America, Abstracts with Programs* **28,** 19.

Kleeman, G. J. and Twist, D. (1989) The compositionally-zoned sheetlike granite pluton of the Bushveld Complex: evidence bearing on the nature of A-type magmatism. *Journal of Petrology* **30,** 1383–1414.

Klepper, M. R., Robinson, G. D. and Smedes, H. W. (1974) Nature of the Boulder Batholith of Montana: Discussion. *Geological Society of America Bulletin* **85,** 1953–1958.

Kress, V. C. and Carmichael, I. S. E. (1991) The compressibility of silicate liquids containing $Fe_2O_3$ and the effect of composition, temperature, oxygen fugacity and pressure on their redox states. *Contributions to Mineralogy and Petrology* **108,** 82–92.

Lange, R. L. and Carmichael, I. S. E. (1990) Thermodynamic properties of silicate liquids with emphasis on density, thermal expansion and compressibility. *Reviews in Mineralogy* **24,** 25–64.

Longhi, J. (1991) Comparative liquidus equilibria of hypersthene-normative basalts at low pressure. *American Mineralogist* **76,** 785–800.

Lynch, H. D. and Morgan, P. (1987) The tensile strength of the lithosphere and the localization of extension. In *Continental Extensional Tectonics*, eds M. P. Coward, J. F. Dewey and P. L. Hancock, pp. 53–65. Geological Society, London Special Publication.

McCaffrey, K. J. W. and Petford, N. (1997) Are granite intrusions scale invariant? *Journal of the Geological Society of London* **154,** 1–4.

McConnell, D. A. and Gilbert, M. C. (1990) Cambrian extensional tectonics and magmatism within the Southern Oklahoma Aulacogen. *Tectonophysics* **174,** 147–157.

Mitchell, J. N., Scoates, J. S. and Frost, C. D. (1995) High-Al gabbros in the Laramie Anorthosite Complex, Wyoming: implications for the composition of melts parental to Proterozoic anorthosite. *Contributions to Mineralogy and Petrology* **119,** 166–180.

Myers, J. D., Gilbert, M. C. and Loiselle, M. C. (1981) Geochemistry of the Cambrian Wichita Granite Group and revisions of its lithostratigraphy. *Oklahoma Geology Notes* **41,** 172–195.

Nakashima, Y. (1993) Static stability and propagation of a fluid-filled edge crack in rock; implication for fluid transport in magmatism and metamorphism. *Journal of Physics of the Earth* **41,** 189–202.

Paterson, S. R., Fowler, T. K., Jr and Miller, R. B. (1996) Pluton emplacment in arcs: a crustal-scale exchange process. *Geological Society of America Special Paper* **315,** 115–126.

Petford, N. (1996) Dykes and diapirs? *Transactions of the Royal Society of Edinburgh, Earth Sciences* **87,** 105–114.

Pollard, D. D. (1973) Derivation and evaluation of a mechanical model for sheet intrusions. *Tectonophysics* **19,** 233–269.

Powell, B. N., Gilbert, M. C. and Fischer, J. F. (1980a) Lithostratigraphic classification of basement rocks of the Wichita Province, Oklahoma. *Geological Society of America Bulletin* **91,** 509–514.

Powell, B. N., Gilbert, M. C. and Fischer, J. F. (1980b) Lithostratigraphic classification of basement rocks of the Wichita province, Oklahoma. *Geological Society of America Bulletin* **91,** 1875–1994.

Powell, B. N., Stockton, M. L., Giddens, J. D. III and Gilbert, M. C. (1982) Stop 3—Hale Spring Locality. In *Geology of the Eastern Wichita Mountains Southwestern Oklahoma*, eds M. C. Gilbert and R. N. Donovan, pp. 102–117. Oklahoma Geological Survey Guidebook, **21**.

Price, J. D., Hogan, J. P. and Gilbert, M. C. (1996a) Rapakivi texture in the Mount Scott Granite, Wichita Mountains, Oklahoma. *European Journal of Mineralogy* **8,** 435–451.

Price, J. D., Hogan, J. P. and Gilbert, M. C. (1996b) Mineralogical variation within the compositionally homogeneous Mount Scott Granite. *Geological Society of America Abstracts with Programs* **28,** 42.

Price, J. D., Hogan, J. P. and Gilbert, M. C. (1996c) Investigation of Late Diabase Dikes at Lake Elmer Thomas Dam. *Geological Society of America Abstracts with Programs* **28,** 42.

Price, J. D., Hogan, J. P., Gilbert, M. C. and Payne, J. (1998) Subsurface and near-surface investigation of the Mount Scott Granite and the Sandy Creek Gabbro, Hale Spring Area, Wichita Mountains, Oklahoma. *Basement Tectonics*, **12** (in press).

Read, H. H. (1948) Granites and granites. In *Origin of Granites*, Geological Society of America Memoir **28** 1–19.

Toplis, M. J., Dingwell, D. B. and Libourel, G. (1994) The effect of phosphorus on the iron redox ratio, viscosity, and density of an evolved ferro-basalt. *Contributions to Mineralogy and Petrology* **117,** 293–304.

Trønnes, R. G. and Brandon, A. D. (1992) Mildly peraluminous high-silica granites in a continental rift: the Drammen and Finnemarka batholiths, Oslo Rift, Norway. *Contributions to Mineralogy and Petrology* **109,** 275–294.

Vander Auwera, J. and Longhi, J. (1994) Experimental study of a jotunite (hypersthene monzodiorite); constraints on the parent magma composition and crystallization conditions ($P$, $T$, $fO_2$) of the Bjerkreim–Sokndal layered intrusion (Norway). *Contributions to Mineralogy and Petrology* **118,** 60–78.

Weaver, B. L. and Gilbert, M. C. (1986) Reconnaissance geochemistry of silicic igneous rocks of the Wichita Mountains, Oklahoma. In *Petrology of the Cambrian Wichita Mountains Igneous Suite*, ed. M. C. Gilbert, pp. 86–106. Oklahoma Geological Survey Guidebook, **23**.

Weertman, J. (1971) Theory of water-filled crevasses in glaciers applied to vertical magma transport beneath oceanic ridges. *Journal of Geophysical Research* **76,** 1171–1183.

Weertman, J. (1980) The stopping of a rising liquid-filled crack in the Earth's crust by a freely slipping horizontal joint. *Journal of Geophysical Research* **85,** 967–976.

Wright, J. E., Hogan, J. P. and Gilbert, M. C. (1996) The southern Oklahoma Aulacogen, not just another B. L. I. P. *EOS Transactions of the American Geophysical Union* **77,** 46, F845.